Step and Flash Imprint Lithography:
A New Approach to High-Resolution Patterning

M. Colburn, S. Johnson, M. Stewart, S. Damle, T. Bailey, B. Choi, M. Wedlake,
T. Michaelson, S.V. Sreenivasan, J. Ekerdt, and C. G. Willson

Texas Materials Institute, The University of Texas at Austin, Austin, TX 78712

ABSTRACT

An alternative approach to lithography is being developed based on a dual-layer imprint scheme. This process has the potential to become a high-throughput means of producing high aspect ratio, high-resolution patterns without projection optics. In this process, a template is created on a standard mask blank by using the patterned chromium as an etch mask to produce high-resolution relief images in the quartz. The etched template and a substrate that has been coated with an organic planarization layer are brought into close proximity. A low-viscosity, photopolymerizable formulation containing organosilicon precursors is introduced into the gap between the two surfaces. The template is then brought into contact with the substrate. The solution that is trapped in the relief structures of the template is photopolymerized by exposure through the backside of the quartz template. The template is separated from the substrate, leaving a UV-cured replica of the relief structure on the planarization layer. Features smaller than 60 nm in size have been reliably produced using this imprinting process. The resulting silicon polymer images are transferred through the planarization layer by anisotropic oxygen reactive ion etching. This paper provides a progress report on our efforts to evaluate the potential of this process.

Keywords: Imprint Lithography

1. INTRODUCTION

Today, 193nm photolithography can produce sub-100nm features using Levenson phase shift masks [1]. A combination of improvements in optics, further reduction in wavelength, and introduction of more complex processes will surely enable printing of still smaller features. Unfortunately, the cost of exposure tools is rapidly increasing, and the cost of the lithographic process is escalating at an enormous rate. The SIA roadmap lists several next generation lithography techniques (NGL) based on ionizing radiation: X-ray, extreme UV, and direct-write e-beam. Each has its advantages and disadvantages, but all are expensive. We seek an inexpensive method of pattern generation capable of sub-100 nm resolution on silicon substrates. If it is to be cheaper, such a process must, by necessity, be very different from those now contemplated.

Philips Research has demonstrated a photopolymer (2-P) process for use in the manufacture of CD-ROMs and DVD disks [2]. In this process, a liquid acrylate formulation is photopolymerized in a glass template to generate the required topographical features. The Philips group has shown that this process is capable of replicating very small features. While the 2-P process shows promise for creating high-resolution images, it does not produce high aspect ratio images, and the patterned acrylate polymers lack the etch resistance required for semiconductor manufacturing. Professor Chou *et al.* at Princeton have demonstrated a compression molding process capable of producing 10 nm features in PMMA. They have also proposed various multilayer techniques for improving the aspect ratio and etch resistance of images generated by compression molding [3]. But as our work and Professor Chou's has shown, this process requires both high pressures and high temperatures [4]. Imprint techniques have also been developed by Whitesides *et al.* that are able to generate intricate patterns on curved surfaces by site specific placement of self assembled monolayers [5, 6, 7]. While these elegant techniques are well suited for specific applications they may not provide a workable means to achieve layer-to-layer overlay at the dimensional tolerance required by next generation device structures. So, we sought to define a new set of materials that, together with a new process, would enable low-cost generation of high-resolution features for use in fabrication of semiconductor devices.

We have previously investigated the prospect of imprinting a silicon thermoplastic at elevated temperatures and pressures. Our goal was to generate a bilayer structure analogous to that produced by bilayer or tri-layer lithographic processes [8]. An organic thermoset planarizing/transfer layer was coated on a silicon wafer and then cured. A thin layer of a silicon-containing

thermoplastic was spin coated on the transfer layer. An etched polysilicon on silicon template was brought into contact with the coated substrate. This "sandwich" structure was then placed in a press and heated to 150 °C under pressure for 15 minutes. An advantage to this process is that one needs only to generate low aspect ratio features. These features can then be transferred through the transfer layer via an anisotropic O_2 RIE etching process analogous to that used in bilayer lithography to generate high aspect ratio, high-resolution images.

Some results from this compression molding process are shown in Figure 1. The micrograph on the left demonstrates the transfer of 2 μm grating features over a large area. The image on the right illustrates a serious problem with this approach. Imprinting with varying pattern density results in incomplete displacement of the thermoplastic even at high temperature and pressure for long times.
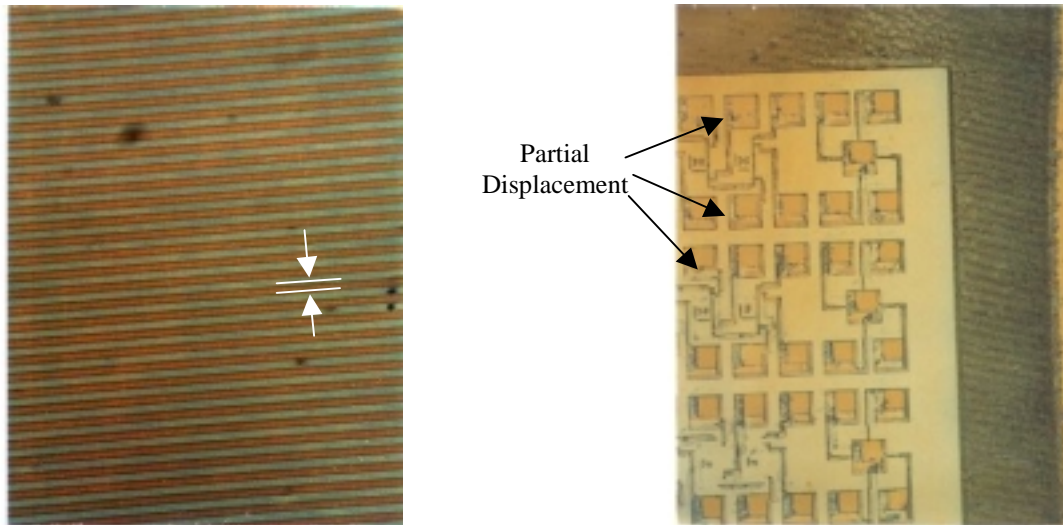

Figure 1. Optical micrograph of a 2 μm grating structure created at 150 ºC at a pressure of 40 psi (left), and a partial displacement of polymer in a pattern with irregular pattern density (right).

Partial pattern transfer, failure to displace material completely, release difficulties, and harsh process conditions seemed to limit the potential of this approach. H.C. Scheer *et al*. also have documented these problems with compression molding of PMMA derivatives [9]. The use of high temperatures and high pressures would severely complicate alignment and overlay issues found in microelectronic device fabrication. Because of our experience and that of others, we choose to refocus our efforts on a different technique that we call "Step and Flash Imprint Lithography" or SFIL.

2. STEP AND FLASH IMPRINT LITHOGRAPHY

In the SFIL process, an organic transfer layer is spin-coated on a silicon substrate. A surface treated, transparent template bearing relief structures of a circuit pattern is closely aligned over the coated silicon substrate. Once in proximity, a drop of a low viscosity, photopolymerizable, organosilicon solution is introduced into the gap between the template and the substrate. The organosilicon fluid fills the gap by capillary action. The gap is closed when the template makes contact with the transfer layer that is coated on the substrate. Once in contact, the structure is irradiated with ultraviolet light through the backside of the template. Ultraviolet exposure cures the photopolymer and creates a solidified, silicon rich, low surface energy replica of the template. Once the photocuring is complete, the template is separated from the substrate leaving a relief image on the surface of the coated substrate. An oxygen-RIE etch through the transfer layer is used to create a high aspect ratio image on the substrate. This process is conducted at room temperature, and since the template is transparent, all of the alignment schemes that have been used successfully in mask aligners can be implemented without difficulty. The unit processes required to create the image are depicted in Figure 2. The process is simple in concept, but every step in the process presents interesting challenges in engineering and materials science. We have begun to explore these challenges and report our progress here.
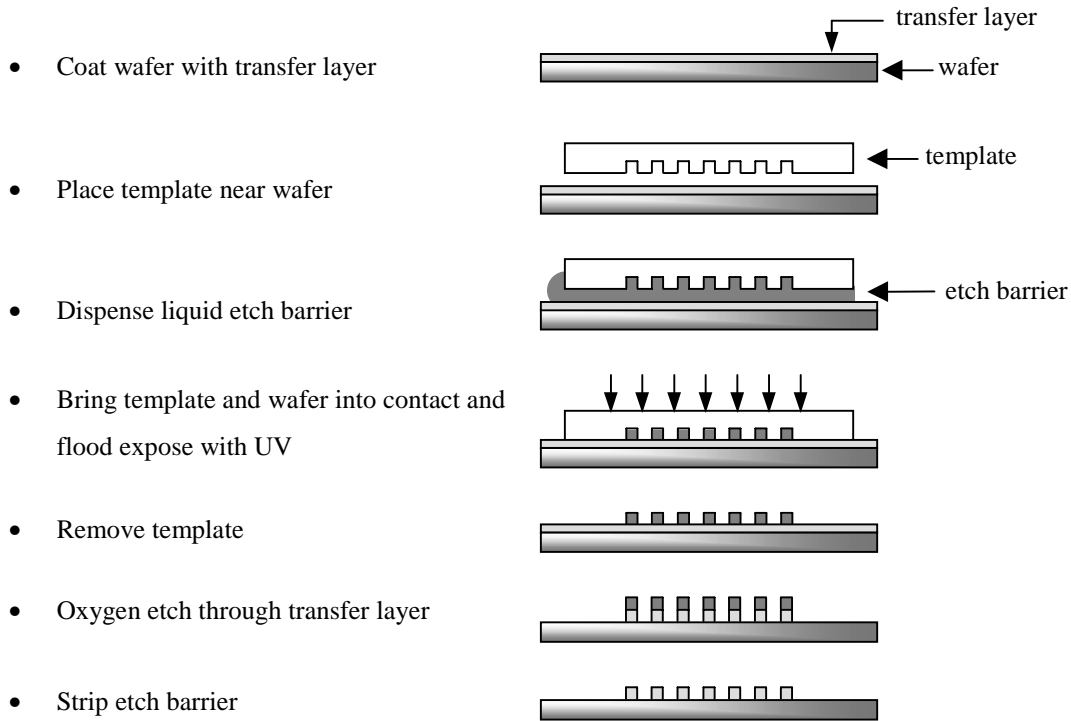
• Coat wafer with transfer layer	
• Place template near wafer	
• Dispense liquid etch barrier	
• Bring template and wafer into contact and flood expose with UV	
• Remove template	
• Oxygen etch through transfer layer	
• Strip etch barrier	

transfer layer

wafer

template

etch barrier

Figure 2. Step and Flash Lithography Process Sequence

2.1   Template

The design and production of a high quality template is key to the success of SFIL. In the early stages of our work, the templates were prepared by patterning chromium on quartz in the standard mask production process. The chromium features were then used as an etch mask to allow generation of relief images in the quartz substrate. The etch process employed was the same one used to make phase shifting masks. Once the etch was complete, the chromium was stripped, and the blanks were cut to fit the holder on the imprint apparatus. This process allowed us to successfully generate high quality 0.35 μm imprints. However, we quickly learned that the resolution of SFIL exceeded the limits of conventional mask technology. We are grateful to International SEMATECH, RTC, and ETEC for their generous contributions to template fabrication.

A set of higher resolution templates has recently been generated for the Step and Flash process by IBM through adaptation of their internal phase-shift mask production process. A 6 in. × 6 in. piece of quartz was coated with chromium and resist, and high resolution test patterns were produced in the resist using electron beam lithography with the 75 keV IBM EL4+ e-beam writer. These patterns were transferred through the chromium and into the quartz via dry etching. The finished 6 in. × 6 in. template was then stripped of chromium and coated with a protective layer of resist. The resist coated quartz template was cut into fifteen individual 1.5 in. × 1.0 in. templates. Each template contains a patterned area that is approximately 130 mm^2. The patterns include images ranging in size from 20 μm to 60 nm. Scanning electron micrographs of selected areas on the etched template are provided in Figure 3. We are now using the first of these templates in our resolution test studies. We are very grateful to IBM for its generous contribution to this study.
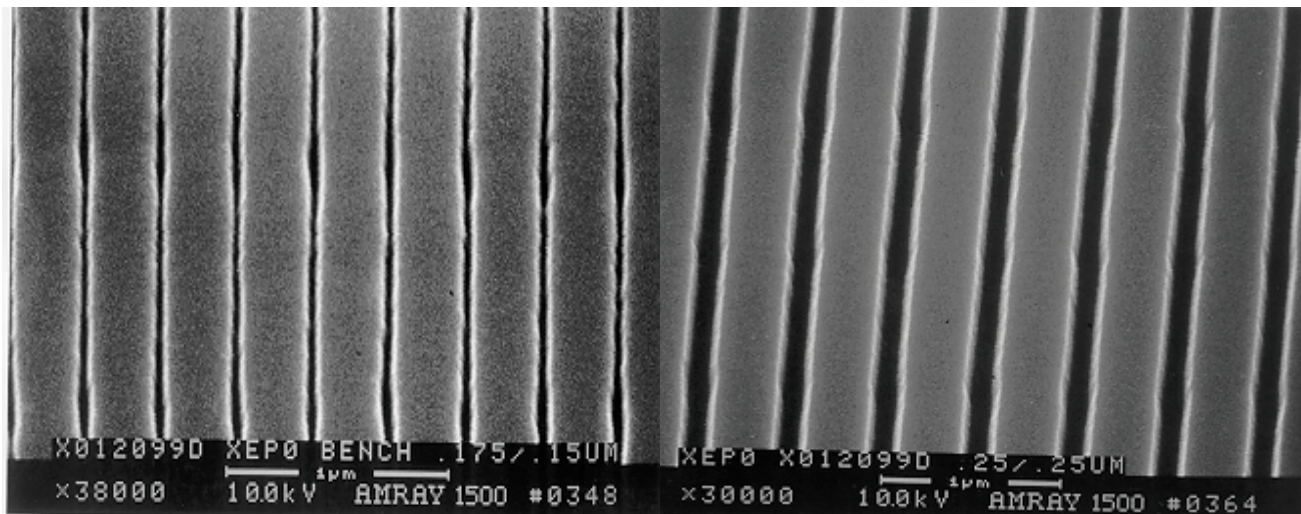
Figure 3. Scanning Electron Micrographs of SFIL Template from IBM. The etched images on the right are 114 nm, nominal, with slightly angled sidewalls; those on the left are 60 nm and represent the resolution limit of the template process as practiced.

Several additional steps were taken to prepare the template for imprinting. The current imprint laboratory is not in a cleanroom environment. Particle contamination issues have made imprinting over the entire 1.5 in. × 1.0 in. template difficult. As a temporary solution, the active area of the template was reduced using the following process. The templates were cleaned thoroughly using a piranha etch followed by a DI water rinse in an ultrasonic bath. An "active" area of the template, approximately 64 mm^2, was identified and isolated by applying a thin layer of a negative photoresist (Olin HR100), with a pipette. The resist was baked for 10 minutes at 90 ℃, and exposed to 114 mJ/cm^2 of light. The active area of the template was thus protected by insolublized resist. The structure was dipped in hydrofluoric acid for approximately 13 minutes to etch the background back by approximately 12 μm, thereby isolating a raised imprint field on the template. The HR100 resist was removed using tetrahydroxyfuran (THF), and the template was re-cleaned using a piranha etch followed by an ultrasonic DI water rinse. After cleaning, the surface was treated with a release layer.

2.2   Release Layer

The surface chemistry of all of the materials must be controlled to insure release at the etch barrier/template interface. The surface energy of the templates was modified by treatment with a release agent. The procedure was carried out in a dry box containing nitrogen. The templates were immersed in a 0.2 wt.% solution of tridecaflouro-1,1,2,2 tetrahydrooctyltrichlorosilane in HFE7100 (from 3M) and allowed to sit for 15 minutes. The trichlorosilanes react with the surface forming covalent bonds to the quartz. After 15 minutes, the templates were removed from the mixture and were rinsed in HFE7100 for 15 minutes to remove unreacted silylating agent and adsorbed layers. The resulting surfaces have excellent releasing properties and are ready to use as imprint templates.

2.3   Transfer Layer material

The ideal organic transfer layer must have several specific characteristics. It must adhere tenaciously to both the silicon wafer and etch barrier. It must function as a planarization layer upon which to imprint, and it must provide high etch rate selectivity during the device etch step. We have not yet focused on the design of an optimum transfer layer. For early testing, we have employed conventional negative tone photoresists because of their ease of use and ready availability. Most of our resolution tests have been conducted using HR 100 from OLIN as the transfer layer.

2.4   Etch Barrier

Several critical issues must be considered in designing the SFIL etch barrier chemistry: adhesion, photopolymerization kinetics, shrinkage, and etch selectivity. We have addressed some of these problems. Tailoring surface properties is crucial.

The etch barrier fluid must wet the template well to facilitate filling of the topography, yet it must release from the template readily after exposure. These requirements are conflicting, and the trade-offs must be analyzed and understood.

Wettability and adhesion (1) are governed by the surface energy of the etch barrier. The rate at which the fluid fills the gap between the substrate and the template has been modeled based on the capillary flow analysis described in the Washburn equation (2). Examination of the Washburn and work of adhesion equations shows that the surface tension must be carefully balanced to produce a workable compromise between ease of release and fast filling time. The work of adhesion (W_{Adh}) is minimized by decreasing the surface energy of the solid/vapor interfaces (γ_a, γ_b) and by increasing that of the solid/solid interface (γ_{ab}). Increasing the surface tension of the fluid, which in turn, is detrimental to the work of adhesion, maximizes the rate of fill. The rate of fill is proportional to H, the gap distance between the template and substrate, and γ_a, the surface tension. It is inversely proportional to R, the radius of curvature of the meniscus, and x, the distance of the meniscus along the length of the capillary.

$$W_{Adh} = \gamma_A + \gamma_B - \gamma_{AB} \qquad (1)$$

$$\frac{dx}{dt} = \frac{(H^2 \gamma_A / R)}{24 \mu x} \qquad (2)$$

Hence, there is a conflict between photopolymerization kinetics and fluid dynamics requirements that poses another complication. The rate of fluid displacement during capillary fill is inversely proportional to the viscosity of the fluid as shown by the Washburn equation. The typical photopolymer fluid contains a blend of functionalized oligomers and reactive diluents. The viscosity of the solution is directly proportional to the oligomer concentration, as is the rate of cure. So, we must consider the trade-off between viscosity and cure speed. Beyond the constraints imposed by kinetics, fluid dynamics, and surface thermodynamics, the etch barrier must provide high etch rate selectivity with respect to the transfer layer during anisotropic oxygen reactive ion etching. We studied the issues required to evaluate this trade-off and have achieved etch selectivity by incorporating silicon into the etch barrier solution.

We formulated our first etch barrier solutions from a free radical generator dissolved in a solution of organic monomer, silylated monomer, and a dimethyl siloxane (DMS) oligomer. Each component serves a specific role in meeting these constraints. The free radical generator initiates polymerization upon exposure to actinic illumination. The organic monomer ensures adequate solubility of the free radical generator and adhesion to the organic transfer layer. The silylated monomers and the DMS provide the silicon required to give a high oxygen etch resistance. Both monomer types help maintain the low viscosity required for filling. The silylated monomer and DMS derivative also serve to lower the surface energy, allowing for template release.

Test formulations were made from a variety of commercially available monomers and DMS derivatives listed in Table 1. These were tested for reactivity and surface energy properties over the range of concentrations listed. The silylated monomers, crosslinking agents, and DMS derivatives were purchased from Gelest, Inc., and used as received. The free radical generators were acquired from Ciba-Giegy Specialty Chemicals Division. The organic monomers were purchased from Aldrich. A statistical response surface optimization procedure was employed to develop the preliminary etch barrier formulations.

Table 1. Components and Range of Compositions Tested as Viable Etch Barrier Solution

Principal Component	Weight Percent	Chemical Names
Monomer	25-50%	Butyl Acylrate, Methyl Acrylate, Methyl Methacrylate
Silylated Monomer	25-50%	Methacryloxypropyl Tris(Tri-Methylsiloxy) Silane (3-Acrylopropyl) Tris(Tri-Methylsiloxy) Silane
Dimethyl Siloxane Deriviative	0-50%	(Acryloxpropyl) Methylsiloxane Dimethylsiloxane Copolymer (Acryloxpropyl) Methylsiloxane Homopolymer Acryloxy Terminated Polydimethylsiloxane
Crosslinking Agent	0-5%	1,3-Bis(3-Methacryloxypropyl)-Tetramethyl Disiloxane
Free Radical Generator	2-10%	Irgacure 184, Irgacure 819

2.5   Imprint Apparatus

We have designed and constructed a test stand for the SFIL process. Illustrated in Figure 4, the machine performs a number of functions during the SFIL process. First, a template is mounted in the template seat and a silicon wafer is placed on the orientation stage. The template seat and orientation stage lie inside a precision positioner constructed of two horizontal plates and linear roller bearings. The roller bearings are preloaded to allow only vertical motion between the template and the wafer.

Figure 4. Step and Flash Lithographic Press

A linear actuator consisting of a brushless DC servo motor, a harmonic drive gear reducer, and a precision ground ball screw slowly lowers the template and positions it directly above the silicon wafer. The servo motor, harmonic drive, and ball screw combination offers motion resolution on the order of 10 um over a range of up to 6 in. The use of a preloaded ball screw nut and harmonic drive eliminates backlash. Once the template is positioned directly above the wafer, the UV curable etch barrier is dispensed and fills the gap between the template and wafer. The linear actuator then lowers the template and presses it against the wafer with controlled force.

Kinematically correct flexures in the orientation stage allow the wafer to orient itself to achieve parallel contact with the template. Figure 5 illustrates the wafer orientation stage. An aluminum flexure ring supports a vacuum chuck in the center of the stage. When a template contacts a wafer on the orientation stage, the template generates a moment about the center of the stage. This moment deflects the flexure ring supporting the vacuum chuck. The circular symmetry of the ring allows the wafer to match the orientation of the template while minimizing lateral motion between the template and wafer. Transducers in the orientation stage monitor contact forces between the template and wafer.
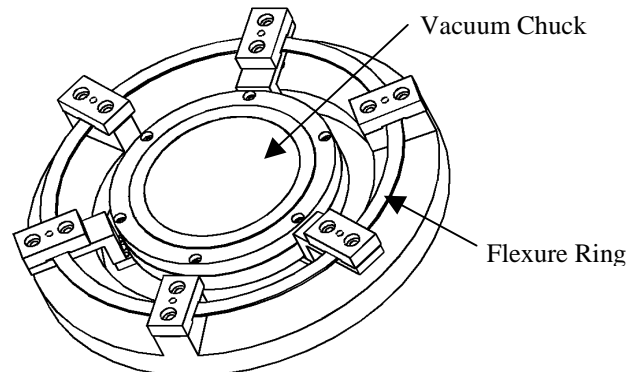

Figure 5. Wafer Orientation Stage

As illustrated in Figure 6, the flexure ring allows the orientation stage to rotate in the alpha and beta directions and translate in the Z direction but it is necessarily very stiff in rotation around the Z axis and translation in the α,β plane. Lateral translations or rotations in the range of nanometers after the cure would shear the images off of the transfer layer. Current image transfer trials use contact forces of less than fifteen pounds force (lb$_f$) that deflect the orientation stage up to a maximum of 2 mm. in the Z direction.
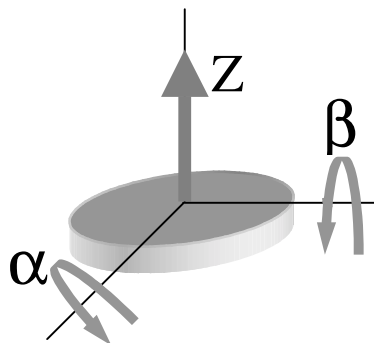

Figure 6. Orientation Stage Degrees of Freedom

After the template and wafer are in parallel contact, ultraviolet light illuminates the etch barrier. An Oriel mercury vapor lamp provides UV light with a peak output near 365 nm. A liquid light guide directs the light into the machine. A lens collimates the light exiting the liquid guide, and a mirror reflects the light onto the template/wafer interface. After the etch barrier crosslinks, the linear actuator separates the template and wafer. The wafer is removed from the machine for inspection and further processing.

3. MATERIAL CHARACTERIZATION

3.1 Photopolymerization Kinetic Studies

High productivity with SFIL will require rapid photopolymerization of the etch barrier. We have therefore set out to establish methods of directly measuring photopolymerization kinetics and will expand these studies to include the time evolution of mechanical properties and surface energy. We have conducted preliminary studies on the kinetics of the photopolymerization curing process using real-time infrared spectroscopy. In this method, the IR absorbance of the polymerizing functional group is monitored while the sample is simultaneously exposed to UV irradiation. As polymerization proceeds, the concentration, and thus absorbance, of the polymerizing functional group decreases. Several variations on this experimental method are described in the literature [10, 11, 12].

We used this technique to screen various potential components for the etch barrier solution to determine their influence on the rate of polymerization and extent of conversion. The IR absorbance band centered around 1640 cm^{-1}, which corresponds to the C=C stretching frequency was used to monitor the reaction of these compounds. The free-radical photoinitiator used was 1-benzoyl-1-hydroxycycloxhexane (Irgacure 184) from Ciba-Geigy. Samples were prepared by placing a drop of the liquid to be studied on a gold-coated silicon wafer. A sodium chloride disc was placed onto the wafer, thereby trapping a thin film of etch barrier solution between the wafer and disc. The sample was then secured inside a nitrogen-purged chamber.

An IR interrogating beam enters the sample chamber through a silicon window. The beam passes through the sample at normal incidence, reflects off the gold-coated substrate, passes directly back through the sample and then to the detector. UV light enters the chamber through a fused silica window, and is directed onto the sample at an angle of approximately 15 degrees off perpendicular. The samples were exposed with broad-band, unfiltered UV light at 3.1 mW/cm^2 intensity. IR spectra of the samples were then rapidly recorded during exposure. The area of the 1640 cm^{-1} absorbance peak was calculated, and conversion was plotted against time. IR absorbance measurements were made with a Nicolet Magna-IR 550 Fourier-transform infrared spectrometer with an external, liquid nitrogen cooled MCT detector from Axiom Analytical. An Oriel Model-66002 mercury lamp equipped with a cold mirror to remove infrared radiation provided UV irradiation.

The ideal etch barrier would polymerize quickly and achieve nearly total conversion of the polymerizing functional group. Our kinetic experiments showed that the etch barrier components we auditioned varied widely in their rate of polymerization.

Variation in extent of conversion among the components was also observed. Figure 7 shows photocuring data for organic and silylated monomers. Of the organic monomers, butyl acrylate and methyl acrylate are both viable candidates for inclusion in the etch barrier solution, but methyl methacrylate is clearly not. Methyl methacrylate's rate of polymerization is much too slow to achieve high conversion during a reasonable exposure time. Figure 7 also shows that butyl acrylate and methyl acrylate both achieve close to total conversion. Hence, our first fluid formulations were based on acrylates. The cure rates for silylated monomers showed a pattern similar to the organic monomers. The cure rate for the acryloxysilane monomer was much greater than that for the methacryloxysilane monomer. Based on these results we have chosen to use acryloxysilanes in our formulations.
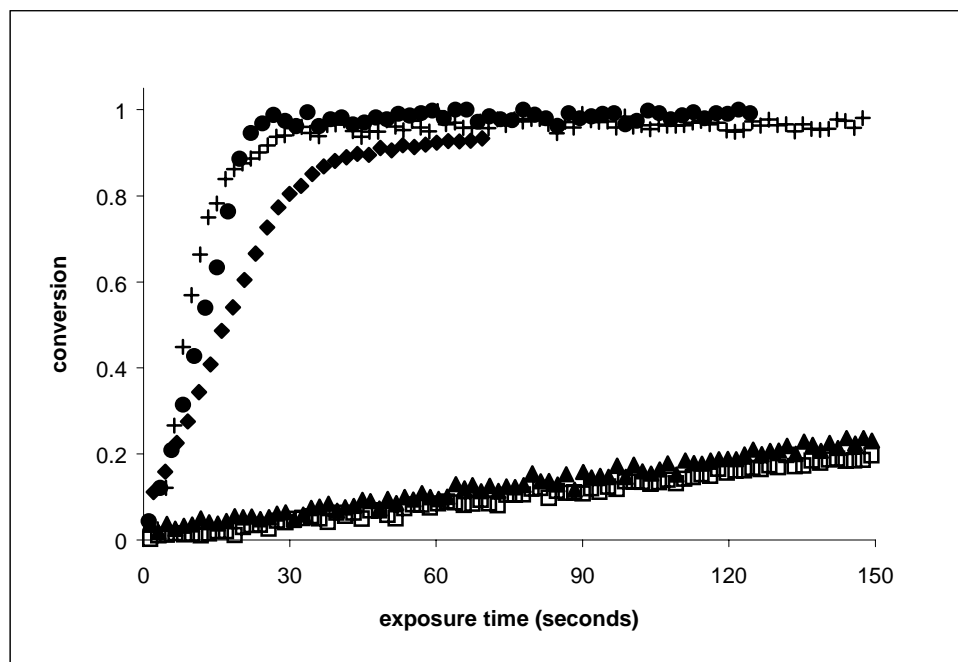

Figure 7. Organic and Silylated Acrylate Monomer Photopolymerization Rates.
butyl acrylate (◆), methyl acrylate (●) methyl methacrylate (▲), acryloxysilane (+), methacryloxysilane (□)

3.2 Surface Characterization

The surface energies of transfer layers and cured etch barriers were calculated using the Acid-Base method developed by van Oss *et al.* [13]. The contact angles of three fluids (water, diiodomethane, and glycerol) were measured on a substrate. The surface energy of the substrate was calculated from these contact angles. Surface tensions were determined using the Pendent Drop Method [14]. In this method, the diameter of a drop is measured at two locations along the length of the drop. Based on the ratio of these diameters, the surface tension of the sample can be extrapolated from a table generated by Andreas *et al*. Measurements were made in an enclosed environmental chamber with controlled temperature and ambient. Samples of pure silylated monomer, pure dimethyl siloxane oligomer, and etch barrier solutions were characterized. Contact angles and surface tensions were measured on a Rame-Hart goniometer equipped with a CCD camera and image analysis software.

The surface tensions of pure silylated monomers and DMS derivatives ranged from 18 to 28 dynes/cm. However, surface tensions of all the formulations are identical, within experimental error, at 25 dynes/cm. This result indicates that the low surface energy components migrate to the liquid/air interface and control the surface tension.

A table of surface energies for several etch barriers that functioned in the process is shown below, together with the data for three transfer layers, an untreated template and a treated template. It should also be noted all three transfer layers have similar predicted adhesion performance with a work of adhesion of 70-75 dynes/cm. The three etch barrier solutions have nearly identical properties. Table 3 presents the work of adhesion between SFIL interfaces. The lowest work of adhesion is at the etch barrier/template interface. These results indicate a preferential release at that interface, as is observed

experimentally. It should be noted that the surface energy of these films was taken on a surface that was in contact with a treated quartz template. As such, the extrapolation of W_{Adh} to the transfer layer may include some error. This error would result in a lower etch barrier/transfer layer interfacial energy, improving the chance of selective release between the etch barrier and the template.

Table 2. Surface Energy of SFIL in dynes/cm.

Material	γ^{p+}	γ^{p-}	γ^p	γ^d	γ^{total}
HR100	0.29	3.47	2.01	39.7	41.7
Poly(vinyl cinnamate)	0.23	13.3	3.50	39.6	43.2
Poly(styrene)	0.74	4.31	3.57	42.3	45.9
Etch Barrier – A	0.17	6.96	2.17	27.8	30.0
Etch Barrier – D	0.03	9.50	1.07	27.9	28.7
Etch Barrier – E	0.06	5.77	1.18	29.9	31.1
Treated Template	1.00	44.2	13.3	9.09	22.3
Untreated Template	3.21	34.4	21.0	28.7	49.7

Table 3. Work of Adhesion between SFIL Interfaces.

Work of Adhesion (dynes/cm)	Etch Barrier A	Etch Barrier D	Etch Barrier E
HR100	71	70	72
Poly(vinyl cinnamate)	72	71	73
Poly(styrene)	75	75	76
Treated Template	42	40	41
Untreated template	71	69	70

Our first pass etch barrier formulation consists of 47 wt.% UMS-182, 3.5 wt.% Irgacure 184, 1.5 wt.% Irgacure 819, 24 wt.% SIA 0210.0, and 24 wt.% butyl acrylate.

Capillary action has been the primary method of introducing the photopolymerizable liquid, but it also has been applied successfully using a drop method and by a spin coating process. In the drop method, a drop of solution is simply placed on the substrate. The template is then brought into contact to expel excess liquid and is subsequently exposed.

3.3 Resolution Evaluation

During resolution evaluation, all patterns were generated using compressive forces between 2 and 15 lbs. Three force transducers located beneath the wafer stage monitored contact forces during the imprint process. A 500W Oriel lamp containing a high pressure bulb having peak intensity at 365 nm provided broadband illumination. Duration of exposure was controlled using an electrically driven shutter. The template released easily without damaging the photopolymerized structure. Using our first pass formulation, we are able to imprint 60 nm features reliably with an exposure dose of 20 mJ/cm^2 and imprint force of 5 lb$_f$. Figure 8 shows a comparison of 60 nm patterns on the IBM template and relief patterns produced on the etch barrier. Figure 9 shows two high-resolution relief patterns; the left highlighting the pattern profile, the other the pattern sidewalls. The resolution of the process is still template limited. Very small imperfections (<10 nm) in the template are accurately reproduced. The process has high resolution and high fidelity. We believe the smallest of structures generated in the template can be accurately replicated by SFIL.
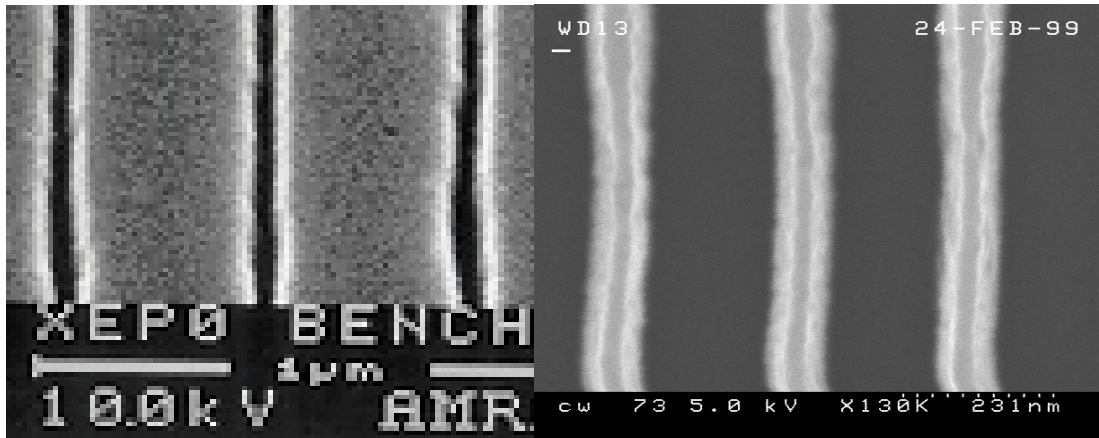
Figure 8. The left SEM micrograph shows the 60 nm images etched into the template generated by IBM. The left micrograph shows a top image of 60 nm relief pattern on the etch barrier.
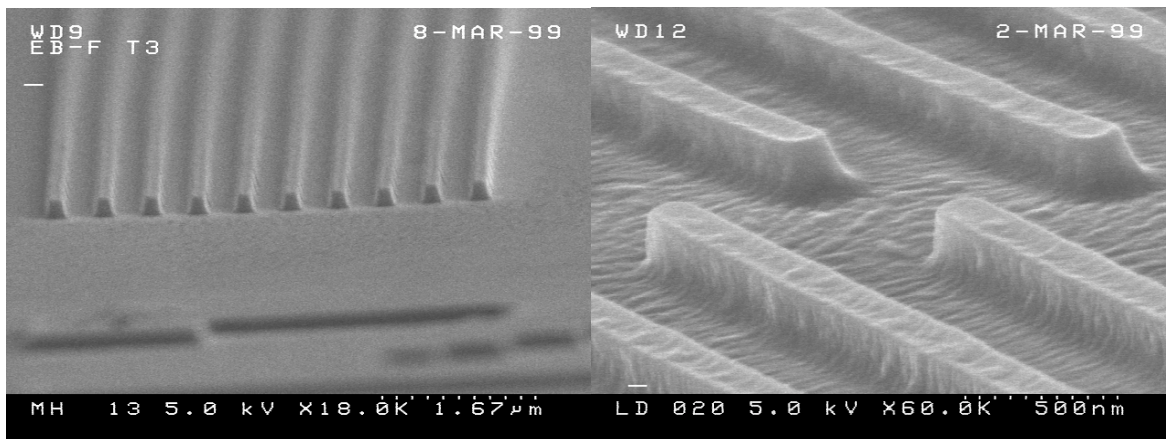

Figure 9. The SEM on the left shows 170 nm features transferred to the etch barrier. The SEM on the right shows the sidewalls on 150 nm features transferred to the etch barrier.

4. CONCLUSIONS

Step and Flash Imprint Lithography appears to have several process advantages over comparable compression imprinting techniques. The SFIL process is implemented at room temperature and requires low pressures only up to 15 psi, while our compression imprinting techniques required temperatures up to 180 ºC, high pressure, and long process times. We have shown that Step and Flash Imprint Lithography has the capability of producing high-resolution topography on a coated substrate. We have formulated solutions that both cure rapidly and release easily. A prototype imprint apparatus has been designed that eliminates image shear during illumination and separation. The process has very high resolution and excellent pattern fidelity. We must now develop the etch sequence required to transfer the pattern to the substrate, and continue to optimize the etch barrier for structural integrity. We will also extend this technique to pattern curved surfaces.

ACKNOWLEDGEMENTS

REFERENCES

1. Patterson, K., Okoroanyanwu, U., Shimokawa, T., Cho, S., Byers, J., Willson, C. G. "Improving Performance of 193 nm Photoresists Based on Alicyclic Polymers," *Proc. SPIE-Int. Soc. Opt. Eng.*, 3333(Pt. 1), 425-437 (1998).

2. Haisma, J.; Verheijen, M.; van der Huevel, K.;van den Berg, J. "Template-assisted nanolithography: A process for reliable pattern replication," *J. Vac. Sci. Technol. B* **1996**, *14*(6), 4124-29.

3. Chou, Stephen; web page: http://www.ee.princeton.edu/~chouweb/

4. Chou, S.Y.; Krauss, P.R.; Renstrom, P.J. "Nanoimprint lithography," *J. Vac. Sci. Technol. B* **1996**, *14*(6), 4129-33.

5. Widden, T.K.; Ferry, D.K.; Kozicki, M.N.; Kim, E.; Kumar, A.; Wilbur J.; Whitesides, G.M. "Pattern Transfer to Silicon by microcontact printing and RIE," *Nanotechnology* **1996,** *7*, 447-451.

6. Xia, Y.; Whitesides, G.M. "Soft Lithography," *Angew. Chem. Int*. **1998**, *37*, 550-575.

7. Wang, D.; Thomas, S.G.; Wang. K.L.; Xia,Y.; Whitesides, G.M. "Nanometer scale patterning and pattern transfer on amorphous Si, crystalline Si, and SiO2 surface using self-assembled monomlayers," *Appl. Phys. Lett*. **1997**, *70* (12).

8. Shaw, J; Babich, E., Hatzakis, M.; Paraszczak, J.J. *Solid State Technology*. **1987**, *6*, 83.

9. Scheer, H-C; Schults, H.; Gottschalch, F.; Hoffmann, T.; Torres, C.M. Sotomayor "Problems of the Nanoimprint Technique for nm-scale Pattern Definition," presented at *EIPBN* **1998**.

10. Decker, C.; Moussa K "Real-Time Monitoring of Ultrafast Curing by UV-Radiation and Laser Beams," *Journal of Coatings Technology*, **1990**, *62*(786), 55-61.

11. Crivello, J.V.; Lai, T.L.; Malik, R. "Ketene Acetal Monomers: Cationic Photopolymerization," *Journal of Polymer Science, Part A: Polym. Chem*. **1996**, *34*, 3103-3120.

12. Bor-Sen Chiou, Saad A. Khan. "Real-Time FTIR and in Situ Rheological Studies on UV curing Kinetics of Thiol-ene Polymers," *Macromolecules*, **1997**, *30* (23), 7322-7328.

13. van Oss, C.J., Good, R.J., Chaudhury, M.K. *J. Colloid Interface Sci.*,**111**, 378 (1986)

14. Andreas, J.M.; Hauser, E.A.; Tucler, W.B., *J. Phys. Chem.*, **1938**, 42, 1001.